Probing the Viability of Oxo-Coupling Pathways in Iridium-Catalyzed Oxygen Evolution

Jonathan Graeupner,[†] *Ulrich Hintermair,*[†#] *Daria L. Huang,*[†] *Julianne M. Thomsen,*[†] *Mike Takase,*[†] *Jesús Campos,*[†] *Sara M. Hashmi,*[§] *Menachem Elimelech,*[§*] *Gary W. Brudvig,*[†*] *and Robert H. Crabtree*[†*]

[†] Department of Chemistry, Yale University, 225 Prospect Street, New Haven, Connecticut 06520, USA.

[§] Department of Chemical and Environmental Engineering, Yale University, 9 Hillhouse Avenue, New Haven, Connecticut 06520, USA.

[#] Centre for Sustainable Chemical Technologies, University of Bath, Bath BA2 7AY, UK.

menachem.elimelech@yale.edu, gary.brudvig@yale.edu, robert.crabtree@yale.edu

ABSTRACT

A series of Cp*Ir^{III} dimers have been synthesized to elucidate the mechanistic viability of radical oxo-coupling pathways in iridium-catalyzed O_2 evolution. The oxidative stability of the precursors toward nanoparticle formation and their oxygen evolution activity have been investigated and compared to suitable monomeric analogues. We found that precursors bearing

monodentate NHC ligands degraded to form nanoparticles (NPs), and accordingly their O_2 evolution rates were not significantly influenced by their nuclearity or distance between the two metals in the dimeric precursors. A doubly chelating bis-pyridine-pyrazolide ligand provided an oxidation-resistant ligand framework that allowed a more meaningful comparison of catalytic performance of dimers with their corresponding monomers. With sodium periodate ($NaIO_4$) as the oxidant, the dimers provided significantly lower O_2 evolution rates per [Ir] than the monomer, suggesting a negative interaction instead of cooperativity in the catalytic cycle. Electrochemical analysis of the dimers further substantiates the notion that no radical oxyl-coupling pathways are accessible. We thus conclude that the alternative path, nucleophilic attack of water on high-valent Ir-oxo species, may be the preferred mechanistic pathway of water-oxidation with these catalysts, and bimolecular oxo-coupling is not a valid mechanistic alternative as in the related ruthenium chemistry, at least in the present system.

Introduction

The attractiveness of water as an alternative fuel source is growing steadily with the growth of worldwide population as well as increase in living standards, which demand increased exploration of solar power.[1,2] One of the key steps in using water as a viable solar fuel is its oxidation to dioxygen and reducing equivalents as shown in eq 1.[3,4]

$$2H_2O \longrightarrow 4H^+ + 4e^- + O_2 \qquad E_{1/2} = 1.23 \text{ V vs NHE at pH} = 0$$

Equation 1. The water-oxidation half-reaction.

Plants, algae, and cyanobacteria oxidize water, using the oxygen evolving complex (OEC), an oxo-bridged Mn_4Ca cluster in the enzyme photosystem II.[5] Despite a growing number of homogeneous water oxidation catalysts utilizing a variety of transition metals (Mn, Fe, Co, Ni, Cu, Ru, Ir),[6-14] a synthetic system combining low overpotentials with high turnover rates and sufficient robustness for large-scale application has yet to be developed.

In 1982, Meyer *et al.* reported a ruthenium dimer as the first homogeneous water oxidation catalyst (WOC), and in 1999 Brudvig and Crabtree described a mangenese terpy dimer.[15,16] One proposed mechanism for water oxidation is radical oxo-coupling (ROC) with the O-O bond formation being the rate-determining step. Based on the analogy with the tetrametallic oxo-cluster in the biological OEC, it was believed that poly-metallic catalysts were generally beneficial for this type of mechanism.[17]

In 2005, however, a series of mono-nuclear Ru-based WOCs were reported, showing that a single metal center can be capable of mediating the water oxidation cycle through nucleophilic attack of water (WNA) on an electrophilic metal-oxo.[18] This finding was followed by Bernhard's report in 2008 on mono-nuclear Ir^{III} complexes as precatalysts for water-oxidation with Ce(IV).[19] Since then, Ir^{III} half-sandwich complexes have been extensively studied as WOCs.[11,12,20-22] Both Cp* (Cp* = pentamethylcyclopentadienyl) and Cp (Cp = cyclopentadienyl) half-sandwich Ir^{III} complexes are viable precatalysts, not only for water-oxidation but also selective CH-oxidations.[23,24] We have used $NaIO_4$ as a primary oxidant in this chemistry because of its ease of handling, good solubility, and lack of absorptions in the visible and near-UV. The disadvantage is that we cannot be certain if the reaction catalyzed in this case is true water oxidation rather than periodate dismutation: $2\ IO_4^- \rightarrow 2\ IO_3^- + O_2$. The analogue to the WNA mechanism would then become a periodate nucleophilic attack (PNA) on the metal oxo. *Hetterscheid* and *Reek*

have proposed such a PNA mechanism for periodate-driven O_2 evolution with [Cp*Ir(NHC)$(OH)_2$] (NHC = N-dimethylimidazolin-2-ylidene) based on DFT calculations.[25] Unfortunately, experimental distinction of these two cases of nucleophilic attack by oxygen isotope labeling is obscured by the fast oxygen exchange of periodate in aqueous solution.[26] The fact that these precursors also evolve O_2 from water using Ce(IV) or electrochemical potentials[12] shows, however, that these catalysts are able to perform true water-oxidation.

In cases where both closed and open shell pathways are accessible, WNA or PNA can be expected to be slower than ROC because higher oxidation states need to be generated to obtain a sufficiently electrophilic oxo that can undergo WNA or PNA. Both WNA and ROC pathways are known to be viable, for instance, for molecular Co- and Ru-based WOCs,[27,28] and in these systems the ligand framework dictates the mechanism by actively favoring or disfavoring bimolecular oxo-coupling. Recent reports on a series of Ru-WOCs demonstrate strongly accelerated catalysis through ligand-enhanced oxo-coupling.[29-31]

In order to correctly interpret mechanistic analyses, however, one has to ascertain the integrity of the precursor. Some WOC precursors have been shown to undergo rapid ligand degradation under reaction conditions to form polymeric species *in-situ*, which in some cases are also active WOCs.[32] It is thus crucial to investigate the fate of the ligands in the catalyst precursor in order to elucidate the mechanism by which a given system operates.

For our Cp^*Ir^{III} precursors, we succeeded in distinguishing homogeneous from heterogeneous water-oxidation catalysts by monitoring the *in-situ* formation of IrO_x material using an electrochemical quartz nanobalance (EQCN)[20] and time-resolved dynamic light scattering (DLS).[33] Based on kinetic analyses and previous DFT calculations, we proposed a mono-nuclear WNA pathway as the preferred mechanism in the homogeneous iridium systems (Figure **1**).[11,12]

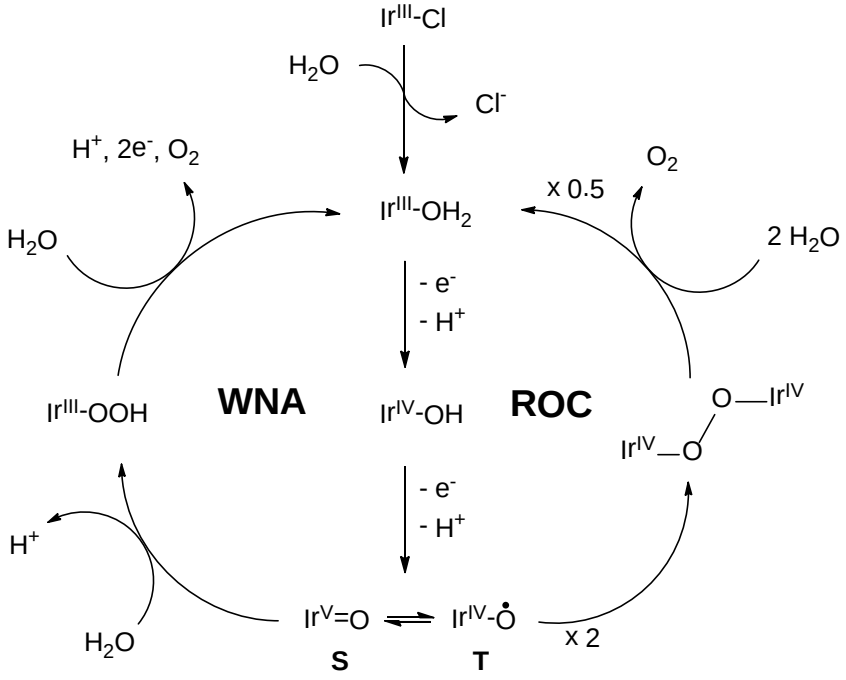

Figure 1. Postulated mechanisms for Ir-catalyzed water-oxidation. Left: Water nucleophilic attack (WNA) on a singlet oxo. Right: radical oxo-coupling (ROC) of two triplet oxo moieties (charges and ligands omitted for clarity)

In the mono-nuclear WNA mechanism, a sequential proton-coupled one-electron oxidation of the Ir^{III} precursor to an Ir^{IV}, and finally a high-valent Ir^{V}-oxo species is proposed. Recent experimental results support these consecutive one-electron oxidation steps through the observation of transient Ir^{IV} species.[34-40] The closed shell Ir^{V}-oxene intermediate subsequently undergoes nucleophilic attack by water leading to the formation of an Ir^{III}-(hydro)peroxide intermediate, which upon further oxidation would dissociate dioxygen and close the catalytic cycle. Computations confirmed the highly electrophilic character of an oxo-unit in an octahedral

Ir^{V}, and the experimental observation of first-order rate dependences on [Ir] suggested a mono-nuclear transformation (plausibly the IV→V oxidation) to be the RDS in these systems.[12,40]

An alternative pathway for the formation of dioxygen might be energetically favorable when two metals are held close together. In this scenario (ROC, Figure **1**), two open-shell Ir-oxyl species could undergo radical coupling leading to the formation of the O-O bond. The reverse of this reaction, the direct oxygenation of two Ir^{III} with O_2 to yield two $Ir^{V}O$, is known for Wilkinson's trimesityl-iridium (doi: 10.1021.ic025700e). For our Cp^*Ir^{III} precursors, WNA barriers were found to be significantly lower on the singlet energy surface by DFT,[12] but ROC barriers can be expected to be lower on the triplet energy surface. Since facile S-T interconversion was found for the formal (V) oxidation state (<5 kcal/mol), both pathways might be accessible through ligand-control as in the related ruthenium chemistry.[29] In Figure **1** only coupling pathways from the formal (V) oxidation state are shown for the sake of simplicity, but other, potentially lower-energy, ROC pathways might be accessible from lower formal oxidation states (i.e., the doublet Ir^{IV}).[41] In order to experimentally probe the viability of ROC mechanisms in Ir-catalyzed WO, we prepared some dimeric Cp^*Ir^{III} precursors and investigated their oxidative stabilities, kinetics in WO catalysis, and electrochemical behaviors, all compared to their respective monomers.

Results and Discussion

Since Cp^*Ir^{III} precursors with NHC ligands are easily accessible and have shown good performance in WOC[42], we first synthesized a series of flexibly linked dimers **2a-d**. Varying the number of methylene groups between the two NHC moieties in the bridging ligands **2a-d** allowed us to vary the distance between the two metals without affecting the electronics.[43]

Figure **3** shows the synthesis of the half-sandwich iridium dimers **2a-d** via transmetalation[44-46] from the corresponding Ag^{I} complexes **1a-d** derived from known bis-imidazolium salts.[43,47]

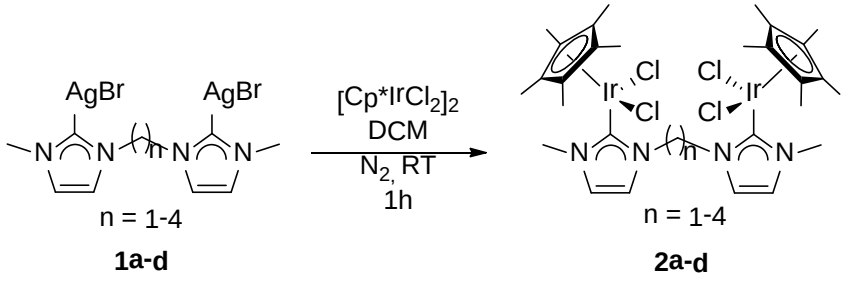

Figure 2. Synthesis of the NHC-linked half-sandwich iridium dimers **2a-d**

Transmetalation of the silver-NHC complexes **1a-d** onto $[Cp^*IrCl_2]_2$ proceeded in nearly quantitative yields in dichloromethane (DCM) at room temperature. Using isolated Ag-NHC complexes with a coordinating halide anion ensured binding of only one NHC moiety per silver to afford stoichiometric NHC donor reagents. This strategy prevents halide abstraction from the iridium precursor and thus suppresses the formation of monomeric by-products with chelating bis-NHC ligands.[48] Due to the presence of different conformers with distinct symmetry in solution, the dimers **2a-d** show two sets of peaks for the bridging NHCs in the NMR spectra. This phenomenon has been observed previously with a variety of bridging ligands with flexible linkers.[43,49-51] The exemplary crystal structure of **2c** shown in Figure 5 confirms the expected connectivity.

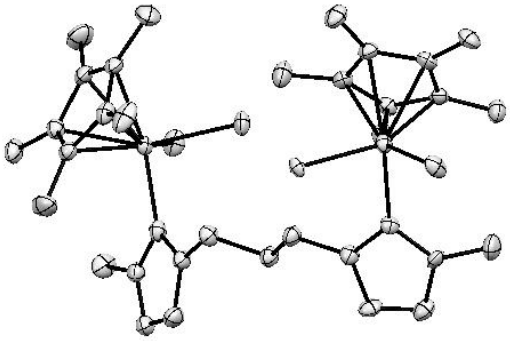

Figure 3. Crystal structure of dimer **2c** (thermal ellipsoids shown at 50 % probability level, hydrogen atoms and CH_2Cl_2 solvent molecules omitted for clarity)

From a simple space model it becomes clear that dimer **2c** in particular would provide an ideal distance between the two iridium centers for oxo-coupling, providing the integrity of the pre-catalyst is retained.

Catalytic activity of oxygen evolution was assessed for complexes **2a-d** using $NaIO_4$ as the oxidant. $NaIO_4$ has been demonstrated to be a superior alternative to CAN (cerium ammonium nitrate, $[NH_4]_2[Ce^{IV}(NO_3)_6]$)[52] because of its mild pH and the absence of potentially seeding precipitates.[53] Activity was measured with a Clarke-type electrode in the liquid phase, and rates were determined from the initial linear regime of O_2 evolution.

Table 1. Rates of catalytic oxygen evolution using Cp*Ir(NHC) precursors[a]

compound	initial rate (μmol O_2 L^{-1} min^{-1})[a]	TOF (min^{-1})
2a, dimer n=1	145.6 ± 9.8	15.7 ± 1.1
2b, dimer n=2	128.4 ± 22.4	14.3 ± 1.9
2c, dimer n=3	164.1 ± 16.8	18.2 ± 2.1
2d, dimer n=4	119.2 ± 18.6	13.2 ± 2.1
3, monomer	224.5 ± 25.0	25.0 ± 5.4

[a] Conditions: 10 µM [Ir], 100 mM $NaIO_4$, 25 ºC (for details see experimental section and the Supporting Information)

As shown in Table **1**, the dimers **2a-d** exhibited rather similar turnover frequencies ranging from 14 min^{-1} to 18 min^{-1}, whereas the monomer **3** (shown in Figure **4**) reached slightly higher rates of ~25 min^{-1}.[54]

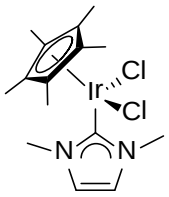

Figure 4 Monomeric Analog **3**

Provided that the NHC ligands were retained throughout the WO cycle, these results would indicate that WNA was largely favored over ROC, and tying two metals together would rather obstruct turnover. In order to test the validity of this data set, we investigated the oxidative stability of the NHC precursors by time-resolved *in-operando* DLS. As can be seen in Figure **5**,

both the dimer **2c** as well as the monomer **3** degraded to form nanoparticles upon oxidation with excess $NaIO_4$ in water. We have previously investigated this behavior in detail and shown that the heterogeneous nano-scale precipitates formed under various conditions originate from the iridium precursors in an oxidative degradation process.[33]

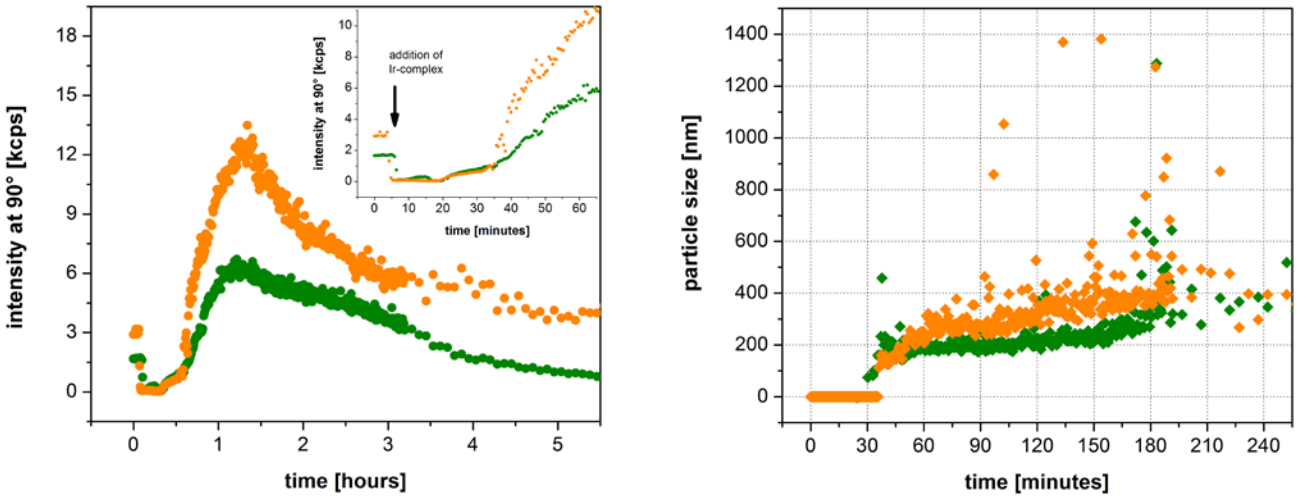

Figure 5. Light scattering intensities and mean particle sizes of diffusional mixtures of complex **3** (orange) or **2c** (green) at 2.5 mM [Ir] with 250 mM $NaIO_4$ in water at room temperature.

Although no heterogeneous material formed during the initial stage of the reaction used for the O_2 evolution kinetics and higher iridium concentrations were required for the DLS measurements, the observation that the active Ir-component ultimately polymerized to oxide NPs strongly suggests complete loss of the organic ligands in the precursors. This observation, coupled with the very similar rates for the different dimers **2a-d** casts doubt on the stability and

utility of monodentate NHC ligands for homogeneous oxidation catalysis. Oxy-functionalization of metal-coordinated NHCs have been observed earlier.[55,56]

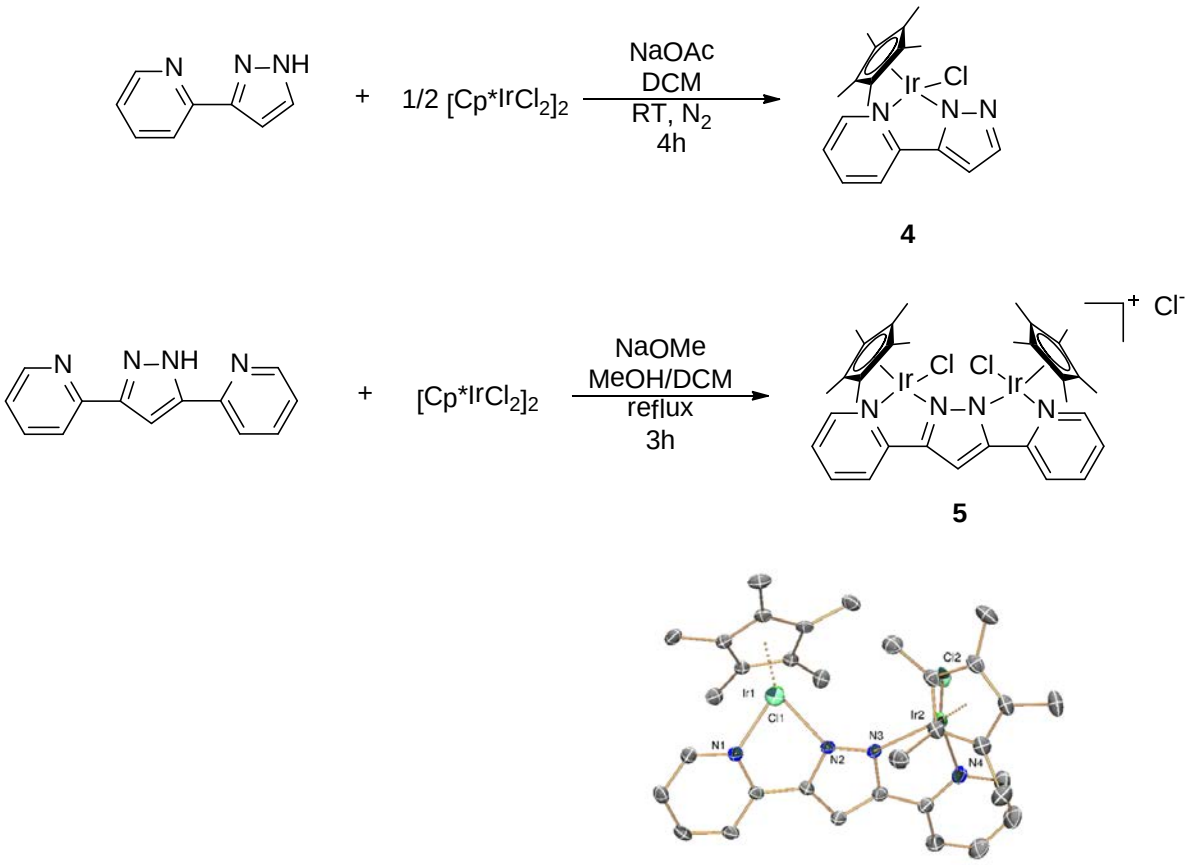

Figure 6a Syntheses of complexes **4** and **5** and crystal structure of **5** (thermal ellipsoids shown at 50% probability, hydrogen atoms and counterion omitted for clarity).

We thus turned to a more robust chelating ligand that would be more stable under reaction conditions to allow studying the effects of nuclearity on WO rates. The doubly chelating bis-pyridine-pyrazolide ligand shown in Figure **6** is known to be an effective framework in ROC water-oxidation with binuclear Ru and Co complexes,[57,58] and synthesis of the Cp*Ir compounds

4 and **5** was straightforward. Assessment of the oxidative stability of the monomer **4** and dimer **5** by time-resolved DLS showed that no heterogeneous material formed under catalytic conditions in this case (Figure **7** and supporting information), suggesting retention of the chelate ligand.

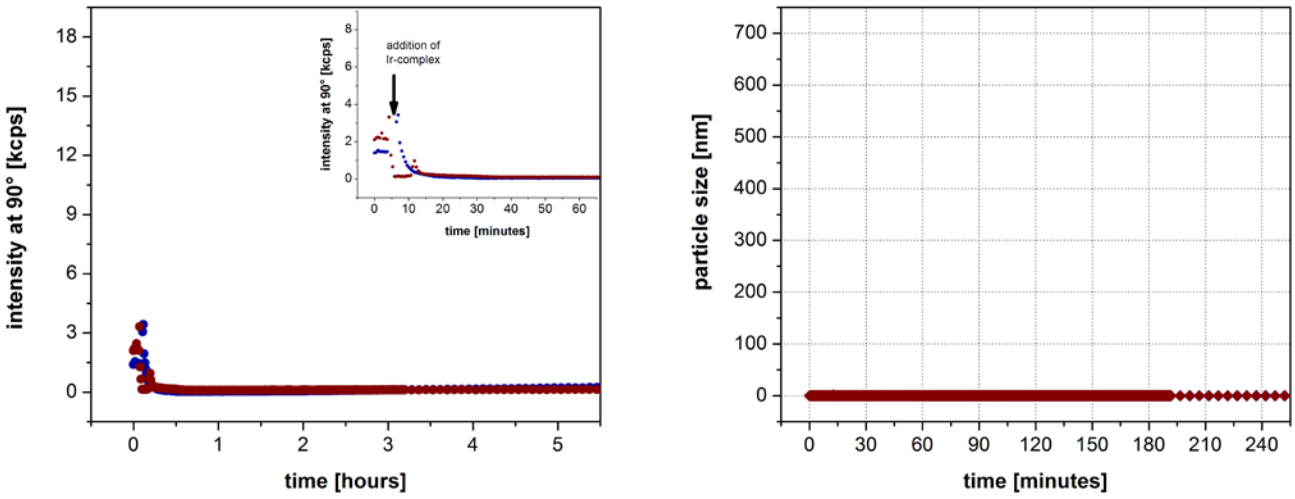

Figure 7. Light scattering intensities and mean particle sizes of diffusional mixtures of complex **4** (red) or **5** (blue) at 2.5 mM [Ir] with 250 mM $NaIO_4$ in water at room temperature.

With a more reliable ligand framework in hand, we compared O_2 evolution rates of monomer **4** and dimer **5** across different iridium concentrations (Figure **8**). Both exhibited a linear rate dependence on [Ir], indicating the RDS to be first order in [Ir] even in the dimer.

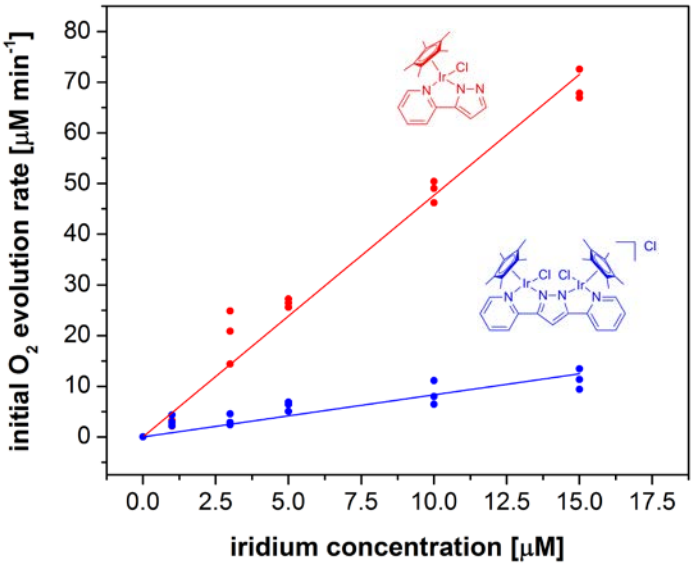

Figure 8. Initial O_2 evolution rates of oxidatively stable monomer **4** (red) and dimer **5** (blue) at various iridium concentrations with 10 mM $NaIO_4$ in water at 25 ºC.

The fact that dimer **5** afforded a first-order rate constant of k_{obs} = 0.83 ± 0.06 min^{-1} whereas the corresponding monomer **4** was almost six times faster on a per metal basis (k_{obs} = 4.77 ± 0.12 min^{-1}) suggests that no cooperative effects prevailed under the conditions applied, and that the two metals rather hinder each other in their individual turnover. To test whether this was due to the formation of stable peroxo species, as reported for a related cobalt dimer,[58] we attempted substitution of the chlorides in **5** with a μ-[O_2] ligand by reaction with Na_2O_2 in an ionizing solvent (Figure **9**). Under the conditions utilized, however, only unreacted starting material could be recovered from these mixtures. This result shows the difficulty of obtaining a stable peroxo Ir^{III}-Ir^{III} species, although the active catalytic species is likely to be different electronically and structurally.[59]

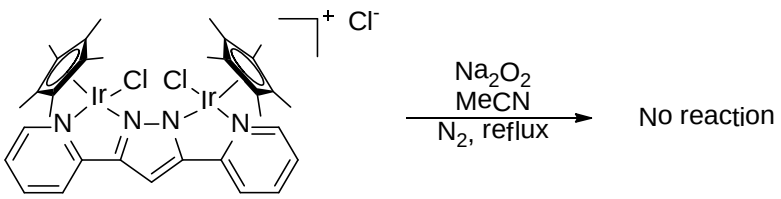

Figure 9 Attempted reaction of **5** with excess sodium peroxide.

To investigate whether the observed detrimental effect of the second metal in dimers of the type of **5** was due to electronic communication, the aqueous electrochemistry of **4** and **5** was assessed by cyclic voltammetry (CV). As can be seen from Figure **10**, no significant differences between monomer and dimer were observed, suggesting that lower oxidation-state ROC pathways are not directly accessible from these precursors.

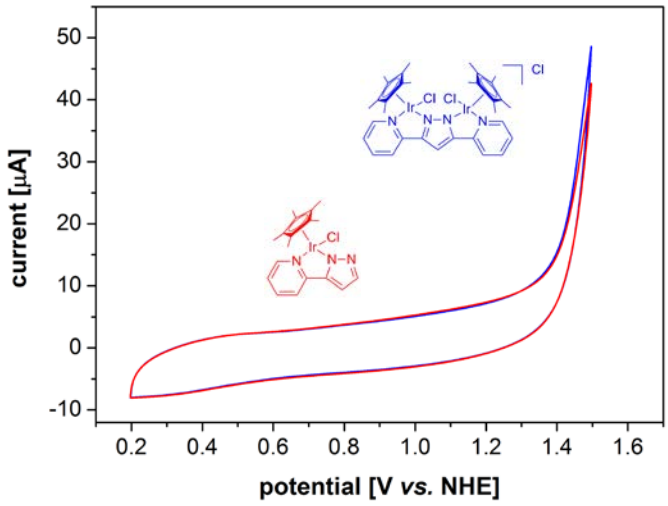

Figure 10. Cyclic voltammograms of **4** (red) and **5** (blue) at 1 mM [Ir] with 100 mV/s in 0.1 M aqueous KNO_3 electrolyte (pH 4) at room temperature (for details see experimental section).

Previous DFT studies predicted an octahedral triplet "Ir^{V}" to have significant spin density on the oxyl ligand,[12] whereas the SOMO of a related doublet Ir^{IV} species was found to be predominantly metal-centered.[35] This might explain why ROC pathways, requiring radical spin density on the oxyl, are not accessible for iridium-based WOCs in the (IV) oxidation state, and suggests that once in the formal (V) oxidation state these systems preferably operate via WNA mechanisms on the singlet energy surface (Figure **1**). The results align well with the observation of stereo-retention in tertiary C-H hydroxylations with the same catalyst system, ruling out radical rebound pathways.

Conclusion

In summary, we report a series of novel Cp^*Ir^{III} dimers linked via monodentate NHCs that degrade to nanoparticles when exposed to $NaIO_4$ in aqueous solution. Accordingly, these dimers show no significant difference in O_2 evolution rates with $NaIO_4$ when compared to an analogous monomer. A novel Cp^*Ir^{III} dimer with an electronically communicating chelate ligand and a suitable monomeric analog were synthesized, showing resistance towards oxidative degradation to NPs under WO conditions. Both follow kinetics that are first-order in [Ir], but the dimer exhibits significantly lower rates for O_2 evolution with $NaIO_4$ as compared to the monomer. The aqueous electrochemistry of both monomer and dimer was found to be virtually identical, in concert indicating that no ROC pathways are accessible for Ir-based WOCs as opposed to Ru- and Co-based systems. Future design of iridium WOCs should therefore focus on WNA mechanisms.

Experimental Section

General All organic solvents were dried using a Grubbs-type purification system. Deionized water was supplied through a centralized purification system (Dept. of Chemistry, Yale University). All chemicals were purchased from major commercial suppliers and used without further purification. $[Cp^*IrCl_2]_2$,[60] $Cp^*Ir(Me_2Im)Cl_2$ (**3**),[54] the bis(imidazolium) ligand precursor salts,[43,47] and the silver NHC complexes **1a-d**[61] were synthesized following literature procedures. NMR spectra were recorded at room temperature on a 400 MHz Bruker or 500 MHz Varian spectrometer and referenced to the residual solvent peak (δ in ppm, J in Hz). Elemental analyses were performed by Robertson Microlit Laboratories (Ledgewood, NJ).

Cp^*Ir^{III}-NHC complexes 2a-d. A 25 mL round-bottomed flask equipped with a stir bar was charged with the appropriate Ag-NHC complex (0.9157 mmol) and $[Cp^*IrCl_2]_2$ (0.869 mmol, 692.2 mg), the mixture evacuated and back-filled with nitrogen. Dry CH_2Cl_2 (10 mL) was added via syringe and the mixture stirred for one hour at room temperature. The resulting mixture was filtered through Celite, the solution reduced to ~5 mL under reduced pressure, and then pentane (50 mL) was added. The resulting yellow-orange precipitate was collected by filtration, washed with pentane (3 x 10 mL), and dried *in vacuo*.

(**2a**) Yield: 803 mg (95%).^{1}H NMR (400 MHz, CD_2Cl_2) δ 7.42 (s, 2H), 7.08 – 7.04 (s, 2H), 6.84 (s, 2H), 3.92 (s, 6H), 1.54 (s, 30H). ^{13}C NMR (126 MHz, CD_2Cl_2) δ 154.3, 124.7, 124.4, 122.6, 89.4, 38.–7, 9.2. Anal. Calc. for $C_{29}H_{42}Cl_4Ir_2N_4$: C, 35.80; H, 4.35; N, 5.76. Found: C, 35.61; H, 4.13; N, 5.79.

(**2b**) Yield: 814 mg (95%). ^{1}H NMR (500 MHz, CD_2Cl_2) δ 8.06 (d, J = 2.0 Hz, 2H), 7.01 (d, J = 2.0 Hz, 2H), 5.13 (d, J = 6.0 Hz, 2H), 4.38 (d, J = 6.0 Hz, 2H), 3.95 (d, J = 1.9 Hz, 6H), 1.56 (s,

30H). ^{13}C NMR (126 MHz, CD_2Cl_2) δ 157.2, 124.1, 123.2, 89.3, 51.6, 38.7, 9.2. Anal. Calc. for $C_{29}H_{42}Cl_4Ir_2N_4$: C, 37.12; H, 4.82; N, 5.59. Found: C, 37.81; H, 4.71; N, 5.33.

(**2c**) Yield: 844 mg (97%).^{1}H NMR (400 MHz, CD_2Cl_2) δ 7.14 (d, *J* = 2.2 Hz, 2H), 6.97 (d, *J* = 2.1 Hz, 2H), 4.77 – 4.66 (m, 2H), 3.91 (d, *J* = 2.3 Hz, 6H), 3.90 – 3.81 (m, 2H), 2.44 (s, 2H), 1.57 (d, *J* = 1.3 Hz, 30H). ^{13}C NMR (126 MHz, CD_2Cl_2) δ 156.1, 124.1, 122.1, 89.0, 47.9, 38.6, 35.9, 9.2. Anal. Calc. for $C_{31}H_{46}Cl_4Ir_2N_4$: C, 37.20; H, 4.63; N, 5.60. Found: C, 36.91; H, 4.63; N, 5.60.

(**2d**) Yield: 846 mg (96%). ^{1}H NMR (400 MHz, CD_2Cl_2) δ 7.16 (d, *J* = 2.4 Hz, 2H), 7.00 (d, *J* = 1.8 Hz, 2H), 4.73 (m, 2H), 3.92 (s, 6H), 3.73 (m, 2H), 1.99 (m, 4H), 1.55 (s, 30H). ^{13}C NMR (101 MHz, CD_2Cl_2) δ 156.6, 123.9, 121.7, 88.9, 50.7, 38.7, 29.5, 9.2. Anal. Calc. for $C_{32}H_{48}Cl_4Ir_2N_4$: C, 37.60; H, 4.77; N, 5.52. Found: C, 37.60; H, 4.53; N, 5.33.

Synthesis of Cp*Ir(pp)Cl (4) $[Cp^*IrCl_2]_2$ (0.5 eqiv., 0.125 mmol, 100 mg), 2-pyrazolylpyridine (1 equiv., 0.251 mmol, 36.4 mg) and NaOAc (6 equiv., 0.753 mmo, 62 mg) are added to a 100 mL Schlenk flask and degassed with nitrogen. 15 mL of dry dichloromethane is added and the reaction is stirred for 3 hours at room temperature. The reaction mixture is then filtered through Celite and the solvent reduced to 5 mL. Excess pentane is added and the resulting precipitate is filtered and washed with pentane to yield a yellow solid. Yield: 121 mg (96%) ^{1}H NMR (400 MHz, CD_2Cl_2) δ 8.55 (ddd, *J* = 5.8, 1.5, 0.8 Hz, 1H), 7.76 (ddd, *J* = 8.1, 7.4, 1.5 Hz, 1H), 7.66 (ddd, *J* = 8.1, 1.5, 0.9 Hz, 1H), 7.60 (d, *J* = 2.0 Hz, 1H), 7.13 (ddd, *J* = 7.3, 5.8, 1.5 Hz, 1H), 6.61 (d, *J* = 2.0 Hz, 1H), 1.72 (s, 15H). ^{13}C NMR (126 MHz, CD_2Cl_2) δ 155.5, 150.5, 148.2, 141.3, 138.6, 122.2, 119.3, 103.0, 87.3, 8.8. Anal. Calc. for $C_{31}H_{46}Cl_4Ir_2N_4$: C, 42.64; H, 4.17; N, 8.29. Found: C, 42.99; H, 3.79; N, 8.12.

Synthesis of $[Cp^*_2Ir_2(bpp)Cl_2]Cl$ (5) $[Cp^*IrCl_2]_2$ (1 equiv., 0.44 mmol, 360 mg) is dissolved in 10 mL degassed dichloromethane and added to a solution of Hbpp (1 equiv., 0.44 mmol, 100 mg) in 10 mL degassed MeOH under N_2. The mixture is heated to reflux for 3 hours. The crude is purified on a neutral silica column. The column is first eluted with acetone to remove a yellow impurity. The product is then eluted using 3% MeOH/DCM. The fractions are collected and the solvent is reduced to 5 mL. Excess pentane is added and the resulting precipitate is filtered and washed with pentane to yield a yellow-orange solid. Yield: 411 mg (95%). ^{1}H NMR (500 MHz, CD_2Cl_2) δ 8.57 (dt, *J* = 5.7, 1.1 Hz, 2H), 8.55 (s, 1H), 8.41 (dt, *J* = 8.0, 1.2 Hz, 2H), 8.03 (td, *J* = 7.8, 1.4 Hz, 2H), 7.49 (ddd, *J* = 7.4, 5.7, 1.4 Hz, 2H), 1.56 (s, 30H). ^{13}C NMR (126 MHz, CD2Cl2) δ 155.0, 150.6, 138.8, 122.7, 121.5, 119.6, 87.5, 8.8. Anal. Calc. for $C_{31}H_{46}Cl_4Ir_2N_4$: C, 47.29; H, 4.14; N, 9.59. Found: C, 46.61; H, 3.98; N, 9.01.

Oxygen Evolution Assays. Oxygen evolution assays were performed as described previously.[12,35] Measurements of O_2 evolution were made with a YSI standard oxygen electrode inserted into a bubble-free, water-cooled jacket at 25 ˚C. In a typical experiment, 5 mL of a freshly prepared solution of $NaIO_4$ (100 mM) were placed in the electrode chamber and left to equilibrate for several minutes. Subsequently, the appropriate volume of aqueous catalyst solution was injected via syringe to start the reaction. The procedure was repeated at least three times to ensure reproducibility.

Dynamic Light Scattering. Light scattering experiments and data analyses were performed as described previously.[33] $NaIO_4$ (1 mmol, 214 mg) was dissolved in water (3 mL) just prior to analysis, and the clear solution passed through a hydrophobic syringe filter (Teflon, 0.2 μm pore size) into the sample vial in the temperature-controlled scattering chamber at 23 °C. New cylindrical screw-cap glass vials (15 × 45 mm) were used for each experiment. The automated

measurement was started, and after collection of a few data points, 1 mL of a filtered aqueous catalyst solution (pH=2.5 with H_2SO_4 in case of **4**) (10 mM in [Ir] = 2.5 mM final [Ir]) was added via syringe to start the reaction. The diffusional mixture was left for the analysis in a dark, undisturbed room.

Electrochemical Studies. Electrochemical Studies. Electrochemical measurements were made on a CH Instruments CHI1200B potentiostat using a standard three-electrode configuration. A glassy carbon electrode (surface area: 0.09 cm^2) was used as the working electrode to minimize background oxidative current. A platinum wire was used as the counter electrode, and a Ag/AgCl reference was used. The measurements were carried out in 0.1 M KNO_3 supporting electrolyte in milli-Q water, and the pH was between 4.3 and 4.5 for all measurements.

Acknowledgements

This material is based in part upon work supported as part of the Argonne-Northwestern Solar Energy Research (ANSER) Center, an Energy Frontier Research Center funded by the U.S. Department of Energy, Office of Science, Office of Basic Energy Sciences under Award Number DE-SC0001059, a catalysis grant from the Division of Chem. Sci.s, Geosciences, and Biosciences, Office of Basic Energy Sciences of the U.S. Department of Energy through grant DE-FG02-84ER13297 and the National Science Foundation under Research Grant CBET-0828795. U.H. thanks the Alexander von Humboldt Foundation for a Feodor Lynen Research Fellowship, supplemented by a grant from the Yale Institute for Nanoscience and Quantum Engineering, and the Centre for Sustainable Chemical Technologies at the University of Bath for a Whorrod Research Fellowship.

Supporting Information

NMR spectra, catalysis data, and crystallographic details. This material is available free of charge via the Internet at http://pubs.acs.org.

References

(1) Lewis, N. S. *Science* **2007**, *315*, 798.
(2) Wild, M.; Gilgen, H.; Roesch, A.; Ohmura, A.; Long, C. N.; Dutton, E. G.; Forgan, B.; Kallis, A.; Russak, V.; Tsvetkov, A. *Science* **2005**, *308*, 847.
(3) Dau, H.; Limberg, C.; Reier, T.; Risch, M.; Roggan, S.; Strasser, P. *ChemCatChem* **2010**, *2*, 724.
(4) Brudvig, G. W. *Philos. Trans. R. Soc. London, Ser. B* **2008**, *363*, 1211.
(5) McEvoy, J. P.; Brudvig, G. W. *Chemical Reviews* **2006**, *106*, 4455.
(6) Concepcion, J. J.; Jurss, J. W.; Templeton, J. L.; Meyer, T. J. *Journal of the American Chemical Society* **2008**, *130*, 16462.
(7) Concepcion, J. J.; Tsai, M.-K.; Muckerman, J. T.; Meyer, T. J. *Journal of the American Chemical Society* **2010**, *132*, 1545.
(8) Fillol, J. L.; Codolà, Z.; Garcia-Bosch, I.; Gómez, L.; Pla, J. J.; Costas, M. *Nat Chem* **2011**, *3*, 807.
(9) Barnett, S. M.; Goldberg, K. I.; Mayer, J. M. *Nat. Chem.* **2012**, *4*, 498.
(10) Liu, X.; Wang, F. *Coordination Chemistry Reviews* **2012**, *256*, 1115.
(11) Hull, J. F.; Balcells, D.; Blakemore, J. D.; Incarvito, C. D.; Eisenstein, O.; Brudvig, G. W.; Crabtree, R. H. *J. Am. Chem. Soc.* **2009**, *131*, 8730.
(12) Blakemore, J. D.; Schley, N. D.; Balcells, D.; Hull, J. F.; Olack, G. W.; Incarvito, C. D.; Eisenstein, O.; Brudvig, G. W.; Crabtree, R. H. *J. Am. Chem. Soc.* **2010**, *132*, 16017.
(13) Savini, A.; Bellachioma, G.; Bolaño, S.; Rocchigiani, L.; Zuccaccia, C.; Zuccaccia, D.; Macchioni, A. *ChemSusChem* **2012**, *5*, 1415.
(14) McEvoy, J. P.; Brudvig, G. W. *Physical Chemistry Chemical Physics* **2004**, *6*, 4754.
(15) Gersten, S. W.; Samuels, G. J.; Meyer, T. J. *J. Am. Chem. Soc.* **1982**, *104*, 4029.
(16) Limburg, J.; Vrettos, J. S.; Liable-Sands, L. M.; Rheingold, A. L.; Crabtree, R. H.; Brudvig, G. W. *Science* **1999**, *283*, 1524.
(17) Romain, S.; Vigara, L.; Llobet, A. *Accounts of Chemical Research* **2009**, *42*, 1944.
(18) Zong, R.; Thummel, R. P. *Journal of the American Chemical Society* **2005**, *127*, 12802.
(19) McDaniel, N. D.; Coughlin, F. J.; Tinker, L. L.; Bernhard, S. *J. Am. Chem. Soc.* **2008**, *130*, 210.
(20) Schley, N. D.; Blakemore, J. D.; Subbaiyan, N. K.; Incarvito, C. D.; D'Souza, F.; Crabtree, R. H.; Brudvig, G. W. *J. Am. Chem. Soc.* **2011**, *133*, 10473.
(21) Lalrempuia, R.; McDaniel, N. D.; Müller-Bunz, H.; Bernhard, S.; Albrecht, M. *Angewandte Chemie International Edition* **2010**, *49*, 9765.
(22) Savini, A.; Bellachioma, G.; Ciancaleoni, G.; Zuccaccia, C.; Zuccaccia, D.; Macchioni, A. *Chemical Communications* **2010**, *46*, 9218.

(23) Zhou, M.; Hintermair, U.; Hashiguchi, B. G.; Parent, A. R.; Hashmi, S. M.; Elimelech, M.; Periana, R. A.; Brudvig, G. W.; Crabtree, R. H. *Organometallics* **2013**, *32*, 957.
(24) Zhou, M.; Schley, N. D.; Crabtree, R. H. *Journal of the American Chemical Society* **2010**, *132*, 12550.
(25) Hetterscheid, D. G. H.; Reek, J. N. H. *European Journal of Inorganic Chemistry* **2013**, n/a.
(26) Pecht, I.; Luz, Z. *J. Am. Chem. Soc.* **1965**, *87*, 4068.
(27) Wasylenko, D. J.; Palmer, R. D.; Berlinguette, C. P. *Chemical Communications* **2013**, *49*, 218.
(28) Hetterscheid, D. G. H.; Reek, J. N. H. *Angewandte Chemie International Edition* **2012**, *51*, 9740.
(29) Maji, S.; Vigara, L.; Cottone, F.; Bozoglian, F.; Benet-Buchholz, J.; Llobet, A. *Angewandte Chemie International Edition* **2012**, *51*, 5967.
(30) Wang, L.; Duan, L.; Stewart, B.; Pu, M.; Liu, J.; Privalov, T.; Sun, L. *Journal of the American Chemical Society* **2012**, *134*, 18868.
(31) Jiang, Y.; Li, F.; Zhang, B.; Li, X.; Wang, X.; Huang, F.; Sun, L. *Angewandte Chemie International Edition* **2013**, *52*, 3398.
(32) Artero, V.; Fontecave, M. *Chem. Soc. Rev.* **2013**, *42*, 2338.
(33) Hintermair, U.; Hashmi, S. M.; Elimelech, M.; Crabtree, R. H. *Journal of the American Chemical Society* **2012**, *134*, 9785.
(34) Graeupner, J.; Brewster, T. P.; Blakemore, J. D.; Schley, N. D.; Thomsen, J. M.; Brudvig, G. W.; Hazari, N.; Crabtree, R. H. *Organometallics* **2012**, *31*, 7158.
(35) Brewster, T. P.; Blakemore, J. D.; Schley, N. D.; Incarvito, C. D.; Hazari, N.; Brudvig, G. W.; Crabtree, R. H. *Organometallics* **2011**, *30*, 965.
(36) De Bruin, B.; Hetterscheid, D. G. H.; Koekkoek, A. J. J.; Grützmacher, H. In *Progress in Inorganic Chemistry*; John Wiley & Sons, Inc.: **2008**, p 247.
(37) Rohde, J.-U.; Lee, W.-T. *Journal of the American Chemical Society* **2009**, *131*, 9162.
(38) Ip, H.-F.; So, Y.-M.; Lee, H. K.; Williams, I. D.; Leung, W.-H. *European Journal of Inorganic Chemistry* **2012**, *2012*, 3289.
(39) Takaoka, A.; Peters, J. C. *Inorganic chemistry* **2011**, *51*, 16.
(40) Savini, A.; Bucci, A.; Bellachioma, G.; Rocchigiani, L.; Zuccaccia, C.; Llobet, A.; Macchioni, A. *European Journal of Inorganic Chemistry* **2013**, n/a.
(41) Polyansky, D. E.; Muckerman, J. T.; Rochford, J.; Zong, R.; Thummel, R. P.; Fujita, E. *Journal of the American Chemical Society* **2011**, *133*, 14649.
(42) Codolà, Z.; M. S. Cardoso, J.; Royo, B.; Costas, M.; Lloret-Fillol, J. *Chemistry – A European Journal* **2013**, *19*, 7203.
(43) Mata, J. A.; Chianese, A. R.; Miecznikowski, J. R.; Poyatos, M.; Peris, E.; Faller, J. W.; Crabtree, R. H. *Organometallics* **2004**, *23*, 1253.
(44) Lee, K. M.; Wang, H. M. J.; Lin, I. J. B. *Journal of the Chemical Society, Dalton Transactions* **2002**, *0*, 2852.
(45) Chiu, P. L.; Chen, C. Y.; Zeng, J. Y.; Lu, C. Y.; Lee, H. M. *Journal of Organometallic Chemistry* **2005**, *690*, 1682.
(46) Wang, H. M. J.; Lin, I. J. B. *Organometallics* **1998**, *17*, 972.
(47) Poyatos, M.; Sanaú, M.; Peris, E. *Inorganic Chemistry* **2003**, *42*, 2572.
(48) Hintermair, U.; Englert, U.; Leitner, W. *Organometallics* **2011**, *30*, 3726.

(49) Herrmann, W. A.; Elison, M.; Fischer, J.; Köcher, C.; Artus, G. R. J. *Chemistry – A European Journal* **1996**, *2*, 772.
(50) Enders, D.; Gielen, H. *Journal of Organometallic Chemistry* **2001**, *617–618*, 70.
(51) Enders, D.; Gielen, H.; Runsink, J.; Breuer, K.; Brode, S.; Boehn, K. *European Journal of Inorganic Chemistry* **1998**, *1998*, 913.
(52) Parent, A. R.; Brewster, T. P.; De Wolf, W.; Crabtree, R. H.; Brudvig, G. W. *Inorg. Chem.* **2012**, *51*, 6147.
(53) Parent, A. R.; Crabtree, R. H.; Brudvig, G. W. *Chemical Society Reviews* **2013**, *42*, 2247.
(54) Hetterscheid, D. G. H.; Reek, J. N. H. *Chemical Communications* **2011**, *47*, 2712.
(55) Herrmann, W. A.; Roesky, P. W.; Elison, M.; Artus, G.; Oefele, K. *Organometallics* **1995**, *14*, 1085.
(56) Hong, D.; Mandal, S.; Yamada, Y.; Lee, Y.-M.; Nam, W.; Llobet, A.; Fukuzumi, S. *Inorganic Chemistry* **2013**, *52*, 9522.
(57) Sens, C.; Romero, I.; Rodríguez, M.; Llobet, A.; Parella, T.; Benet-Buchholz, J. *Journal of the American Chemical Society* **2004**, *126*, 7798.
(58) Rigsby, M. L.; Mandal, S.; Nam, W.; Spencer, L. C.; Llobet, A.; Stahl, S. S. *Chemical Science* **2012**, *3*, 3058.
(59) Hintermair, U.; Sheehan, S. W.; Parent, A. R.; Ess, D. H.; Richens, D. T.; Vaccaro, P. H.; Brudvig, G. W.; Crabtree, R. H. *Journal of the American Chemical Society* **2013**, *135*, 10837.
(60) Ball, R. G.; Graham, W. A. G.; Heinekey, D. M.; Hoyano, J. K.; McMaster, A. D.; Mattson, B. M.; Michel, S. T. *Inorganic Chemistry* **1990**, *29*, 2023.
(61) Gil-Rubio, J.; Cámara, V.; Bautista, D.; Vicente, J. *Organometallics* **2012**, *31*, 5414.

TOC ABSTRACT

The synthesis of Ir dimers with both flexible and rigid ligands is described and their catalytic activity in periodate-driven oxygen evolution is assessed and compared to suitable monomeric analogs. Furthermore, their stability under catalytic conditions and their electrochemical behavior is described.

TOC GRAPHIC